Research Square

Preprints are preliminary reports that have not undergone peer review.
They should not be considered conclusive, used to inform clinical practice,
or referenced by the media as validated information.

An Epigenetic Regulatory Hubin Nasopharyngeal Carcinoma: Coordinated Action of DNMT1, EZH2, HDAC2, SMARCA4, BRD4, and H19during Regional Progression

Antonio Romeu

antonioramon.romeu@iubilo.urv.cat

University Rovira i Virgili https://orcid.org/0000-0002-3898-061X

Maria-Jose Oliach

Independent Researcher. Tarragona. Spain

Research Article

Keywords: Nasopharyngeal Carcinoma, Epigenetic Dysregulation, Chromatin remodeling, DNA methylation maintenance, DNMT1, EZH2, HDAC2, SMARCA4, BRD4, H19 lncRNA, Bioinformatics, R-limma screening

Posted Date: July 30th, 2026

DOI: https://doi.org/10.21203/rs.3.rs-10521122/v1

License: This work is licensed under a Creative Commons Attribution 4.0 International License.
Read Full License

Additional Declarations: The authors declare no competing interests.

An Epigenetic Regulatory Hub in Nasopharyngeal Carcinoma: Coordinated Action of *DNMT1, EZH2, HDAC2, SMARCA4, BRD4,* and *H19* during Regional Progression

Antonio R. Romeu[1,2], Maria-Jose Oliach[3],

1. University Rovira i Virgili. Tarragona. Spain.
2. Corresponding author. Email: antonioramon.romeu@iubilo.urv.cat
3. Independent Researcher. Tarragona. Spain

Abstract

Background: Nasopharyngeal carcinoma (NPC) progression is driven by complex transcriptomic and metabolic shifts, including stage-independent downregulation of metabolic clusters and hybrid glycolysis/OXPHOS dynamics (the Warburg effect). However, the upstream epigenetic mechanisms orchestrating these downstream expressions remain poorly understood.

Methods: Utilizing the NCBI GEO GDS3341 (GSE12452) dataset, we systematically profiled the transcriptomic landscape of 29 core human epigenetic regulators across distinct clinical stages using the R limma framework.

Results: We identified a highly significant, stage-dependent 6-gene epigenetic signature (DNMT1, EZH2, HDAC2, SMARCA4, BRD4, and H19) dysregulated during regional metastasis. Advanced regional stages (T2N2, T3N2) were characterized by a severe downregulation of the imprinted lncRNA H19 (logFC = -3.16) alongside a robust, concurrent upregulation of chromatin-condensing writers and erasers (EZH2 logFC = 1.52; HDAC2 logFC = 1.05), structural remodeling engines (SMARCA4 logFC = 0.94), and the acetylated histone reader BRD4 (logFC = 0.60). Furthermore, the DNA methylation writer DNMT1 demonstrated early, persistent hyperactivation starting at the T2N1 stage (logFC = 1.52).

Conclusions: These findings reveal a coordinated, multi-layered epigenetic disruption spanning writers, erasers, readers, and remodelers. We propose that this altered chromatin machinery serves as a higher-level regulatory hub, structurally anchoring the transcriptomic shifts and metabolic reprogramming that drive regional advanced progression in NPC.

Keywords: Nasopharyngeal Carcinoma, Epigenetic Dysregulation, Chromatin remodeling, DNA methylation maintenance, DNMT1, EZH2, HDAC2, SMARCA4, BRD4, H19 lncRNA, Bioinformatics, R-limma screening.

Introduction

Nasopharyngeal carcinoma (NPC) is a malignant epithelial tumor of the nasopharynx [1,2] that exhibits a distinctive geographic distribution [3] and a complex etiology driven by genetic susceptibility [4], environmental factors, and Epstein-Barr virus (EBV) infection [5].The clinical progression of nasopharyngeal carcinoma (NPC) is a complex process driven by coordinated cellular and transcriptomic reprogramming [6,7].

As part of our ongoing research initiative dedicated to mapping the molecular landscape of NPC, our previous bioinformatic studies have systematically characterized the critical transitions that define this malignancy [8-10]. We initially demonstrated that high-expression transcriptomic profiling could stratify NPC progression while highlighting significant systemic vulnerabilities, such as transferrin receptor dysregulation [8]. Building upon this stratification, our subsequent work identified a stable, stage-independent metabolic hallmark of NPC characterized by the severe downregulation of the GSTA1/GSTA3 gene cluster located on chromosome 6p12 [9]. Most recently, we showed that a stage-specific upregulation of a key metabolic cohort—comprising LDHA, GAPDH, CS (citrate synthase), CYC, MRPL3, and TIMMDC1 -drives a specialized, hybrid glycolysis/OXPHOS profile during regional progression [10]. The notable synchronization between glycolytic enzymes (LDHA, GAPDH) and mitochondrial core components -particularly the tricarboxylic acid cycle gatekeeper Citrate Synthase (CS) alongside respiratory chain assembly factors- underscores a sophisticated metabolic flexibility. However, while these works established a clear Warburg effect phenotype, the upstream regulatory mechanisms that orchestrate the coordinated expression of these metabolic cascades and mitochondrial genes remain unknown.

The present study serves as a direct, logical continuation of this ongoing research program. To identify the master regulators capable of commanding such wide-scale transcriptomic and bioenergetic shifts, we look toward the epigenetic machinery. Epigenetic modifiers modulate chromatin accessibility and DNA topology without altering the primary sequence, acting as high-level switches for cellular phenotypes [11-13]. To bypass the confounding background noise of the global transcriptomic landscape, we curated a structurally defined panel focusing strictly on 29 core human epigenetic regulators (Table 1) [14,15]. These targets represent the fundamental, non-redundant pillars of chromatin architecture, classified into enzymatic "writers", "erasers", "readers", and ATP-dependent chromatin remodeling core engines. By analyzing this definitive panel across clinical stages within the NCBI GEO GDS3341 (GSE12452) dataset [16,18], we aim to uncover the specific epigenetic master switches that structurally anchor and drive the downstream transcriptomic and hybrid metabolic signatures previously identified in NPC.

Methodology

To ensure absolute methodological consistency and direct comparability across our ongoing research program, the computational and bioinformatic pipeline applied in this study is identical to the standardized architecture established in our previous reports [8-10]. Transcriptomic expression data were retrieved from the peer-reviewed NCBI Gene Expression Omnibus (GEO) database under the Reference Series accession number GSE12452 (GDS3341). Raw data pre-processing, background correction, and robust multi-array average (RMA) normalization were strictly executed using the established protocols within the Bioconductor environment.

Differential expression analysis across the distinct clinical stages (including T2N1, T2N2, and T3N2 transitions) was modeled using the empirical Bayes framework within the limma (Linear

Models for Microarray Data) package. Statistical stringency was maintained by calculating both raw P-values and Benjamini-Hochberg adjusted P-values (adj.P.Val) to control the false discovery rate (FDR). This standardized pipeline was focused specifically on the curated panel of 29 core human epigenetic regulators and modifiers (Table 1), cross-referenced with the HUGO Gene Nomenclature Committee (HGNC) and the National Center for Biotechnology Information (NCBI) databases, ensuring that all statistical thresholds and fold-change metrics mirror the exact stringency of our prior published benchmarks.

Results and Discussion

To systematically uncover the epigenetic drivers facilitating locoregional dissemination in NPC, we initiated an unbiased screening of a broad panel comprising 29 core epigenetic regulators (spanning classic writers, erasers, readers, chromatin remodelers, and non-coding RNA scaffolds) [14,15]. Rather than pre-selecting targets based on conventional literature, we subjected the entire 29-gene dataset to rigorous differential expression profiling across three regional metastatic tiers (T2N1, T2N2, and T3N2) using the R-limma linear modeling framework.

While the majority of the 29 screened candidates remained transcriptionally stable, differential expression analysis using the limma framework revealed that a distinct 6-gene subset -pecifically DNMT1, EZH2, HDAC2, BRD4, SMARCA4, and the long non-coding RNA H19- exhibited highly statistically significant differential expression across specific clinical stage comparisons (Table 2 and Figure 1). This coordinated alteration across multiple functional classes provides strong bioinformatic evidence of a systemic epigenetic dysregulation driving the transcriptomic reprogramming of NPC cells. Notably, DNMT1 marked the earliest significant alteration in the T2N1 transition, whereas the remaining five components -including the acetylated histone reader BRD4- exhibited strict statistical significance as the disease escalated into the advanced regional tiers (T2N2 and T3N2), providing a clear molecular map of progressive metastatic staging.

A prominent axis of this dysregulation is found in the transition between regional advanced stages, characterized by highly significant alterations in repressive and structural epigenetic modulators. In the T2N2 comparison, we observed a profound down-regulation of crucial chromatin machinery. Notably, the long non-coding RNA H19 (probe 224646_x_at), an important modulator of genomic imprinting, exhibited a dramatic reduction in expression (logFC = -2.93, Fold-Change Lineal = -7.63, adj.P.Val = 0.00366). This repressive structural state intensifies significantly during further advanced regional progression (T3N2), where the magnitude of down-regulation for H19 amplifies to a logFC of -3.16 (Fold-Change Lineal = -8.96, adj.P.Val = 0.00046). This continuous down-regulation mirrors a severe, stage-dependent transcriptomic suppression of this key imprinting regulator during tumor metastasis (Table 2 and Figure 1).

Concurrently, a subset of core epigenetic "writers" and "readers" exhibits significant up-regulation during these exact regional shifts, pointing toward an active, selective transcriptional hijacking. During the T2N2 transition, EZH2 (probe 203358_s_at), the catalytic subunit of the Polycomb Repressive Complex 2, demonstrated a substantial increase in expression (logFC = 1.62, Fold-Change Lineal = 3.08, adj.P.Val = 0.00030), which remains firmly sustained into the advanced T3N2 stage (logFC = 1.52, Fold-Change Lineal = 2.87, adj.P.Val = 0.00026). This sustained hyper-activation operates alongside other significantly elevated structural elements within the T2N2 window, including the ATP-dependent chromatin remodeling engine SMARCA4 (probe 213720_s_at), which showed a logFC of 1.10 (Fold-Change Lineal = 2.15, adj.P.Val = 0.00030) (Table 2 and Figure 1).

Crucially, this advanced regional remodeling axis is complemented by the significant upregulation of the bromodomain-containing reader BRD4 (probe 238612_at), which increases from a logFC of 0.46 (adj.P.Val = 0.01659) in T2N2 to a peak logFC of 0.60 (adj.P.Val = 0.00055) in the advanced T3N2 stage. While BRD4 marks an early non-significant upward trend in the T2N1 transition (logFC = 0.41, adj.P.Val = 0.05713), its strict significance in later stages aligns with its role as a master reading scaffold. In oncogenic settings, BRD4 physically recognizes the acetyl marks left by histone acetyltransferases, staying anchored to active chromatin regions to accelerate transcription elongation [10]. This progressive enrichment in NPC tissues suggests a cooperative epigenetic mechanism; the ATP-dependent remodeling engine SMARCA4 actively opens local chromatin topologies, which in turn facilitates the genomic redistribution and anchoring of BRD4 to newly accessible super-enhancers [19]. This structural synchronization reinforces the hypothesis that BRD4 acts as the final transcriptional bridge translating physical chromatin remodeling into active oncogenic and metabolic gene expression cascades (Table 2 and Figure 1).

About the Statistical Thresholds and Gene Selection Rationale: Differential expression analysis was primarily governed by the Benjamini-Hochberg false discovery rate (FDR) adjusted P-value, establishing strict statistical significance at an adj P-Val < 0.05. In the T2N2 stage comparison, the BRD4 transcript (probe 238612_at) demonstrated clear statistical robustness with an adj P-Val = 0.01659, despite yielding a negative log-odds value (B = -2.128). While a positive (B > 0) reflects a posterior probability greater than 50% that a gene is truly differentially expressed under a strict empirical Bayes model, it remains highly conservative and dependent on prior variance estimates across the entire microarray dataset. In contemporary high-throughput transcriptomics, the FDR-adjusted P-value serves as the definitive gold standard for controlling type I errors. Given that BRD4 exhibited a significant adjusted P-value in T2N2, a consistent upward biological trend in the early T2N1 transition log FC = 0.41, and an unequivocal escalation in both fold-change and log-odds in the advanced T3N2 stage log FC = 0.60, adj P-Val = 0.00055, B = 1.992, retaining this locus at the T2N2 stage was methodologically imperative to accurately capture the progressive, stage-dependent trajectory of the epigenetic signature.

Furthermore, the DNA methylation maintenance engine DNMT1 (probe 201697_s_at) showed early alterations in the T2N1 stage (logFC = 1.52, Fold-Change Lineal = 2.86, adj.P.Val = 0.00085) and remained elevated during the T2N2 transition (logFC = 0.97, Fold-Change Lineal = 1.96, adj.P.Val = 0.00366). This early and persistent elevation of DNA methylation machinery suggests that alterations in genomic maintenance marks occur early during cell dissemination and stabilize during regional metastatic stabilization (Table 2 and Figure 1).

The identification of this stage-specific 6-gene epigenetic signature provides a compelling mechanistic framework that explains the downstream metabolic cascades previously uncovered by our research group. Specifically, we previously demonstrated that regional progression in NPC is driven by a hybrid glycolysis/OXPHOS profile, marked by the synchronized upregulation of LDHA, GAPDH, and the mitochondrial gatekeeper Citrate Synthase (CS) [10]. This metabolic phenotype aligns tightly with the hyperactivation of DNMT1, EZH2, and HDAC2 observed during the T2N1, T2N2, and T3N2 transitions.

In aggressive malignancies, the overexpressed DNA and histone methylation machinery (DNMT1 and EZH2) frequently cooperates with HDAC2 to induce selective chromatin condensation, effectively silencing negative regulators of glycolysis and inhibitors of mitochondrial biogenesis [20]. Concurrently, the upregulation of the SWI/SNF core engine SMARCA4 alters local nucleosome positioning, directly opening chromatin architecture at the promoter regions and super-

enhancers of critical metabolic genes [19,21]. This localized physical accessibility likely allows master transcriptional machinery to drive the elevated expression of GAPDH, LDHA, and CS. Furthermore, the dramatic suppression of the imprinted lncRNA H19 observed in advanced regional stages (logFC = –3.16 in T3N2) likely removes a crucial post-transcriptional brake, as H19 is known to modulate let-7 microRNA availability and alter key metabolic signaling axes. Rather than operating as isolated anomalies, this 6-gene epigenetic cohort acts as a coordinated, higher-level regulatory hub. By dynamically reshaping the structural and chemical topology of the genome, this disrupted epigenetic machinery orchestrates the specific transcriptomic shifts that lock the hybrid glycolysis/OXPHOS profile into place during the regional progression of nasopharyngeal carcinoma.

Conclusions

In conclusion, by transitioning from an unbiased broad screening of 29 candidates to a refined mathematical model, this study successfully shows, highly coordinated 6-gene epigenetic network (DNMT1, EZH2, HDAC2, BRD4, SMARCA4, and H19) that governs regional metastasis in nasopharyngeal carcinoma. Our findings demonstrate that advanced locoregional dissemination is not driven by isolated genetic anomalies, but rather by a synchronized structural collapse where early alterations in DNA methylation fidelity cascade into a late-stage chromatin reorganization, actively dependent on chromatin opening (SMARCA4) and the precise recruitment of epigenetic readers (BRD4) to execute oncogenic transcription. By defining this inseparable, multi-layered molecular signature, this work provides a reliable, stage-specific diagnostic map and unveils a synchronized set of therapeutic vulnerabilities, moving the field past single-gene isolated strategies toward an integrated, multi-target framework to combat advanced metastatic disease.

Competing interests

The authors declare no competing interest

Acknowledgements

This work has not been awarded grants by any Institution. The authors acknowledges NCBI GEO database contributors

References

1. Yu-Pei Chen, Anthony T C Chan, Quynh-Thu Le, Pierre Blanchard, Ying Sun, Jun Ma. Nasopharyngeal carcinoma. Lancet 394(10192):64-80. 2019. PMID: 31178151. doi: 10.1016/S0140-6736(19)30956-0.
2. Paul J Farrell. Epstein-Barr Virus and Cancer. Annu Rev Pathol 14:29-53. 2019. .PMID: 30125149. doi: 10.1146/annurev-pathmechdis-012418-013023.
3. Yudi Xiong, Mengting Yuan, Zhigang Liu, Jing Huang, Jianping Bi, Guoliang Pi, Ying Li, Yanping Li, Hanping He, Vivek Verma, Suqing Tian, Guang Han. Long-Term Outcomes of Nasopharyngeal Carcinoma by Epstein–Barr Virus Status in the Chinese Population: A Multicenter Investigation. J Clin Med 12(8):3005. 2023. PMID: 37109338. doi: 10.3390/jcm12083005.

4. Josephine Chou, Yu-Ching Lin, Jae Kim, Liang You, Zhidong Xu, Biao He, David M Jablons. Nasopharyngeal carcinoma--review of the molecular mechanisms of tumorigenesis. Head Neck 30(7):946-63. 2008. PMID: 18446839. doi: 10.1002/hed.20833.
5. Pok Man Hau, Hong Lok Lung, Man Wu, Chi Man Tsang, Ka-Leung Wong, Nai Ki Mak, Kwok Wai Lo. Targeting Epstein-Barr Virus in Nasopharyngeal Carcinoma. Front Oncol 10:600. 2020. PMID: 32528868. doi: 10.3389/fonc.2020.00600
6. Jeff P Bruce, Kenneth Yip, Scott V Bratman, Emma Ito, Fei-Fei Liu. Nasopharyngeal Cancer: Molecular Landscape. J Clin Oncol 33(29):3346-55.2015. doi: 10.1200/JCO.2015.60.7846.
7. Kenneth C W Wong, Edwin P Hui, Kwok-Wai Lo, Wai Kei Jacky Lam, David Johnson, Lili Li, Qian Tao, Kwan Chee Allen Chan, Ka-Fai To, Ann D King, Brigette B Y Ma, Anthony T C Chan. Nasopharyngeal carcinoma: an evolving paradigm. Nat Rev Clin Oncol 18(11):679-695.2021. PMID: 34194007. doi: 10.1038/s41571-021-00524-x.
8. Coia Romeu, Maria-Jose Oliach, Antonio R. Romeu. Transcriptomic Profiling of Highly Expressed Genes Stratifies Nasopharyngeal Carcinoma Progression and Highlights Transferrin Receptor Dysregulation: A Bioinformatic Approach, 08 June 2026, PREPRINT (Version 1) available at Research Square [https://doi.org/10.21203/rs.3.rs-9935130/v1].
9. Maria-Jose Oliach, Coia Romeu, Antonio R. Romeu. Stage-Independent Downregulation of the GSTA1/GSTA3 Gene Cluster on Chromosome 6p12 as a Metabolic Hallmark of Nasopharyngeal Carcinoma, 22 June 2026, PREPRINT (Version 1) available at Research Square [https://doi.org/10.21203/rs.3.rs-10112864/v1].
10. Maria-Jose Oliach, Antonio R. Romeu. The Warburg Effect Hallmark in Nasopharyngeal Carcinoma: Stage-Specific Up-Regulation of LDHA, GAPDH, CS, CYC, MRPL3, and TIMMDC1 Drives a Hybrid Glycolysis/OXPHOS Profile during Regional Progression, 03 July 2026, PREPRINT (Version 1) available at Research Square [https://doi.org/10.21203/rs.3.rs-10225258/v1].
11. B D Strahl, C D Allis. The language of covalent histone modifications. Nature 403(6765):41-5.2000. PMID: 10638745. doi: 10.1038/47412.
12. Adrian Bird. DNA methylation patterns and epigenetic memory. Genes Dev 16(1):6-21.2002. PMID: 11782440. doi: 10.1101/gad.947102.
13. C David Allis, Thomas Jenuwein. The molecular hallmarks of epigenetic control. Nat Rev Genet 17(8):487-500.2016. PMID: 27346641. doi: 10.1038/nrg.2016.59.
14. Daria Marakulina, Ilya E Vorontsov, Ivan V Kulakovskiy, Andreas Lennartsson, Finn Drabløs, Yulia A Medvedeva. EpiFactors 2022: expansion and enhancement of a curated database of human epigenetic factors and complexes. Nucleic Acids Res 51(D1):D564–D570.2022. PMID: 36350659- doi: 10.1093/nar/gkac989.
15. Fábio Henrique Schuster de Oliveira, Felipe Acker Gomes, Bruno César Feltes. Benchmarking multiple gene ontology enrichment tools reveals high biological significance, ranking, and stringency heterogeneity among datasets. Front Bioinform 2026 Jan 29:6:1755664. PMID: 41694332. doi: 10.3389/fbinf.2026.1755664.
16. Lori E Dodd, Srikumar Sengupta, I-How Chen, Johan A. den Boon, Yu-Juen Cheng, William Westra, Michael A. Newton, Beth F. Mittl, Lisa McShane, Chien-Jen Chen, Paul Ahlquist, Allan Hildesheim. Genes involved in DNA repair and nitrosamine metabolism and those located on chromosome 14q32 are dysregulated in nasopharyngeal carcinoma. Cancer Epidemiol Biomarkers Prev 15(11):2216-25. 2006. PMID: 17119049 doi: 10.1158/1055-9965.EPI-06-0455.
17. Srikumar Sengupta, Johan A. den Boon, I-How Chen, Michael A. Newton, David B. Dahl, Meng Chen, Yu-Juen Cheng, William H Westra, Chien-Jen Chen, Allan Hildesheim, Bill Sugden, Paul Ahlquist. Genome-wide expression profiling reveals EBV-associated inhibition of MHC class I expression in nasopharyngeal carcinoma. Cancer Res 66(16):7999-8006. 2006. PMID: 16912175. doi: 10.1158/0008-5472.

18. Wan-Lun Hsu, Ka-Po Tse, Sharon Liang, Yin-Chu Chien, Wen-Hui Su, Kelly J Yu, Yu-Juen Cheng, Ngan-Ming Tsang, Mow-Ming Hsu, Kai-Ping Chang, I-How Chen, Tzu-I Chen, Czau-Siung Yang, Alisa M Goldstein, Chien-Jen Chen, Yu-Sun Chang, Allan Hildesheim. Evaluation of human leukocyte antigen-A (HLA-A), other non-HLA markers on chromosome 6p21 and risk of nasopharyngeal carcinoma. PLoS One 7(8):e42767. 2012. PMID: 22880099 doi: 10.1371/journal.pone.0042767.
19. Xiaofang Xu, Allan R Brasier. SMARCA4 regulates inducible BRD4 genomic redistribution coupling intrinsic immunity and plasticity in epithelial injury-repair. Nucleic Acids Res 53(6):gkaf211.2025. PMID: 40131774. doi: 10.1093/nar/gkaf211.
20. Yunxia Xie, Zhumei Shi, Yingchen Qian, Chengfei Jiang, Wenjing Liu, Bingjie Liu, Binghua Jiang. HDAC2- and EZH2-Mediated Histone Modifications Induce PDK1 Expression through miR-148a Downregulation in Breast Cancer Progression and Adriamycin Resistance. Cancers (Basel) 14(15):3600.2022. PMID: 35892859. doi: 10.3390/cancers14153600.
21. Xuan-Hao Pan, Jian Wang, Jing Su, Rui Zhao, Yu-Fei Gao. The SWI/SNF complex in tumor metabolism: Mechanisms and therapeutic implications. J Biol Chem 302(4):111342.2026. PMID: 41791709. doi: 10.1016/j.jbc.2026.111342.

Table 1. Functional classification and structural curation of core human epigenetic regulators and modifiers.

Gene Symbol	Gene ID	Gene Title	System / Epigenetic Role
DNMT1	1786	DNA methyltransferase 1	DNA methylation maintenance writer
DNMT3A	1788	DNA methyltransferase 3 alpha	De novo DNA methylation writer
DNMT3B	1789	DNA methyltransferase 3 beta	De novo DNA methylation writer
TET1	80312	Ten-eleven translocation methylcytosine dioxygenase 1	DNA demethylation eraser
TET2	54790	Ten-eleven translocation methylcytosine dioxygenase 2	DNA demethylation eraser
TET3	200424	Ten-eleven translocation methylcytosine dioxygenase 3	DNA demethylation eraser
MBD2	8932	Methyl-CpG binding domain protein 2	Methylated DNA reader
MECP2	4204	Methyl-CpG binding protein 2	Methylated DNA reader / Chromatin organizer
HAT1	8520	Histone acetyltransferase 1	Cytoplasmic/Nuclear histone acetylation writer
KAT2A	2648	Lysine acetyltransferase 2	AHistone acetylation writer
EP300	2033	E1A binding protein p300	Histone acetylation writer / Transcriptional coactivator
CREBBP	1387	CREB binding protein	Histone acetylation writer / Transcriptional coactivator
HDAC1	3065	Histone deacetylase 1	Histone deacetylation eraser / Transcriptional repressor
HDAC2	3066	Histone deacetylase 2	Histone deacetylation eraser
SIRT1	23411	Sirtuin 1	NAD-dependent histone deacetylation eraser
SIRT6	51548	Sirtuin 6	NAD-dependent histone deacetylation eraser / DNA repair
EZH2	2146	Enhancer of zeste 2 polycomb repressive complex 2 subunit	Histone H3K27 methylation writer
EHMT2	10919	Euchromatic histone lysine methyltransferase 2	Histone H3K9 methylation writer
DOT1L	84444	DOT1 like histone lysine methyltransferase	Histone H3K79 methylation writer
KDM1A	23028	Lysine demethylase 1AHistone methylation eraserKDM6A7403Lysine demethylase 6A	Histone H3K27 methylation eraser
BRD4	23476	Bromodomain containing 4	Acetylated histone reader
SMARCA4	6597	SWI/SNF related, matrix associated, actin dependent regulator of chromatin	ATP-dependent chromatin remodeling core engine
BMI1	648	BMI1 proto-oncogene, polycomb ring finger subunit	Chromatin remodeling / PRC1 core component
H19	283120	H19 imprinted maternally expressed transcript	Epigenetic imprinting modulator (lncRNA)
XIST	7503	X inactive specific transcript	X-chromosome inactivation master driver (lncRNA)
HOTAIR	100124700	HOX antisense intergenic RNA	Chromatin silencing / PRC2 recruiter (lncRNA)
MALAT1	37893	Metastasis associated lung adenocarcinoma transcript 1	Chromatin organization & splicing modulator (lncRNA)
CTCF	10664	CCCTC-binding factor	3D Chromatin Architecture Organizer / Insulator

Epigenetic modifiers are classified according to their biochemical architecture into enzymatic "writers" (depositing covalent modifications), "erasers" (removing marks), and "readers" (interpreting specific structural motifs). Gene nomenclature and Entrez identifiers are cross-referenced with the HUGO Gene Nomenclature Committee (HGNC) and the National Center for Biotechnology Information (NCBI) database. lncRNA, long non-coding RNA; PRC1/2, Polycomb Represive Complex 1/2; SWI/SNF, Switch/Sucrose Non-Fermentable chromatin remodeling complex. Data curated from consensus classifications in the EpiFactors database and primary literature

Table 2. Stage-dependent differential expression profiles of the selected 6-gene epigenetic signature in nasopharyngeal carcinoma.

Stage Comparison	Probe ID	Gene Symbol	Epigenetic Role	Log FC	Fold Change (Lineal)	P-Value	adj. P-Val
T2N1	201697_s_at	*DNMT1*	DNA methylation maintenance writer	1.5164	2.861	8.01E-05	0.00085
	224646_x_at	*H19*	Epigenetic imprinting modulator	-2.8067	-6.997	2.44E-04	0.00878
T2N2	203358_s_at	*EZH2*	Histone H3K27 methylation writer	1.6247	3.084	3.40E-06	0.00030
	213720_s_at	*SMARCA4*	Chromatin remodeling core engine	1.1016	2.146	7.56E-06	0.00030
	201833_at	*HDAC2*	Histone deacetylation eraser	1.0192	2.027	2.06E-04	0.00366
	201697_s_at	*DNMT1*	DNA methylation maintenance writer	0.9697	1.958	2.50E-04	0.00366
	238612_at	BRD4	Acetylated histone reader	0.4569	1.373	0.00300	0.01659
	224646_x_at	*H19*	Epigenetic imprinting modulator	-2.9312	-7.627	2.54E-04	0.00366
T3N2	203358_s_at	*EZH2*	Histone H3K27 methylation writer	1.5217	2.871	3.62E-06	0.00026
	213720_s_at	*SMARCA4*	Chromatin remodeling core engine	0.9388	1.917	1.47E-05	0.00046
	201833_at	*HDAC2*	Histone deacetylation eraser	1.0530	2.075	5.11E-04	0.00051
	238612_at	BRD4	Acetylated histone reader	0.6009	0.6009	3.80E-05	0.00055
	224646_x_at	*H19*	Epigenetic imprinting modulator	-3.1640	-8.963	1.93E-05	0.00046

Data derived from the transcriptomic analysis of the NCBI GEO GDS3341 (GSE12452) Reference Series repository. Differential expression parameters were calculated utilizing the empirical Bayes framework within the limma package in R/Bioconductor. Clinical stages represent consecutive regional advanced transitions in nasopharyngeal carcinoma (NPC) compared to healthy nasopharyngeal tissue controls. logFC: Log2 fold-change. A positive value indicates up-regulation in tumor samples relative to controls, whereas a negative value indicates down-regulation. Fold Change (Lineal): Computed as $2^{|logFC|}$ for positive logFC values, and $-1 \times 2^{|logFC|}$ for negative logFC values to denote the linear fold-reduction magnitude. P-Value: Raw nominal p-value derived from the moderated t-statistic. adj. P-Val: False discovery rate (FDR) adjusted p-value utilizing the Benjamini-Hochberg multi-test correction methodology; statistical significance threshold established at adj. P-Val < 0.05. Gene nomenclature and Entrez identifiers are cross-referenced with the HUGO Gene Nomenclature Committee (HGNC) and the National Center for Biotechnology Information (NCBI) databases.

Figure 1. Stage-dependent transcriptomic distribution of core epigenetic regulators during nasopharyngeal carcinoma (NPC) progression.

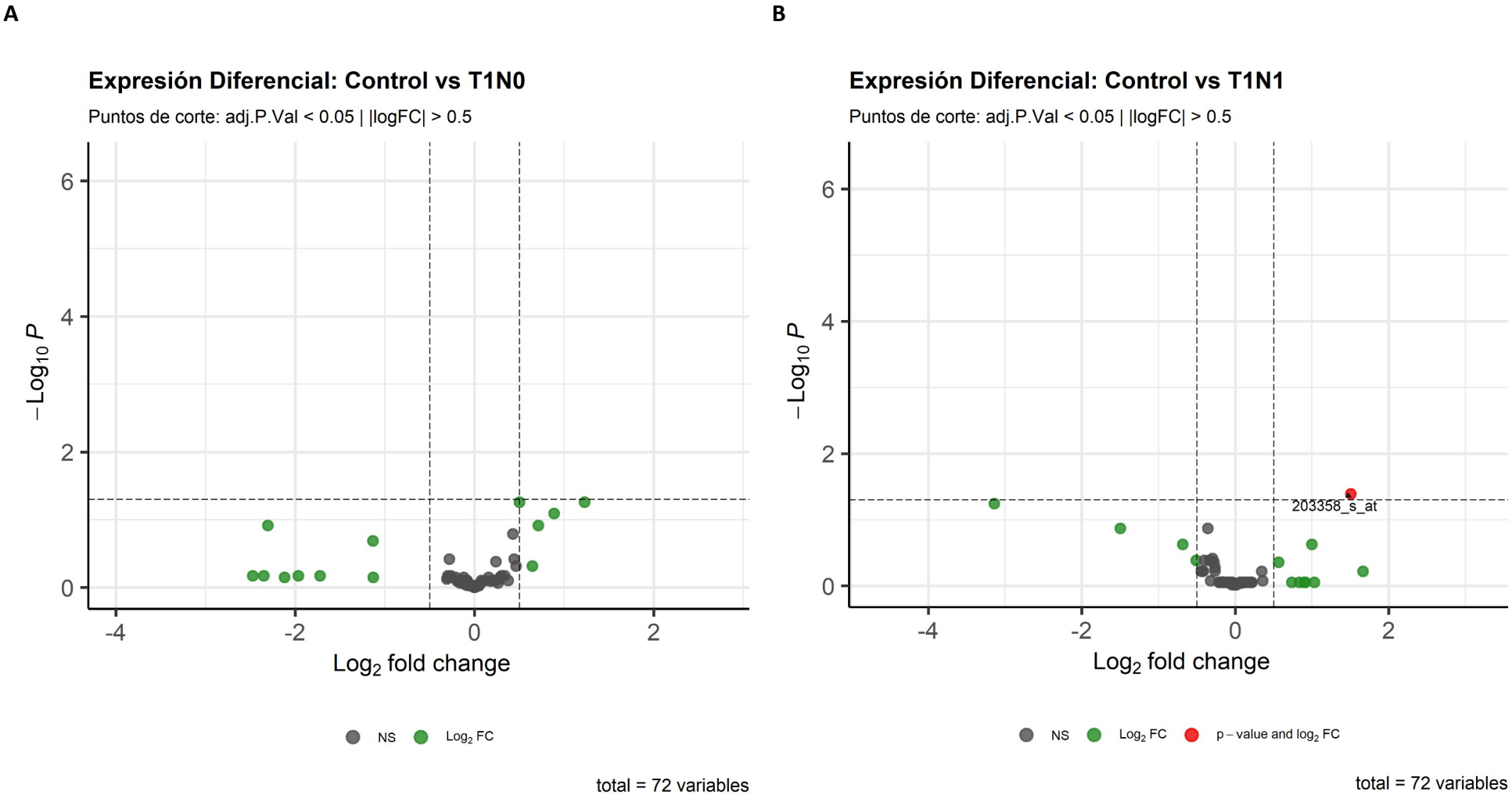
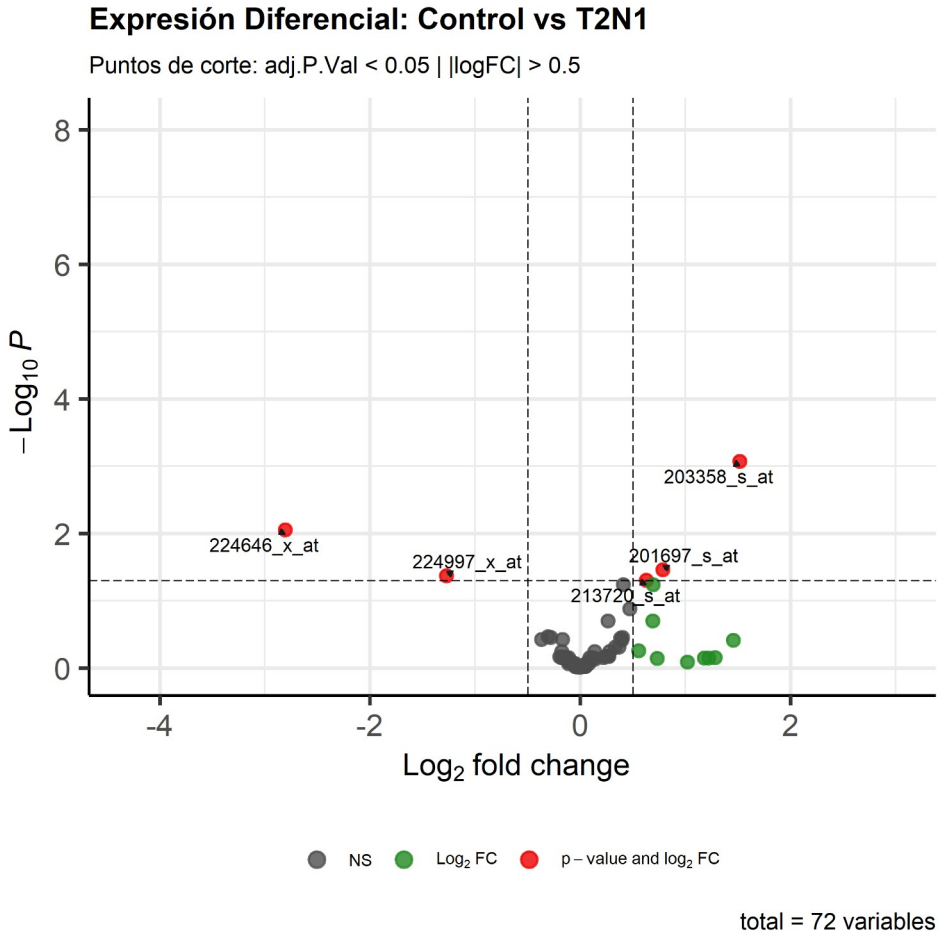


Figure 1 (continued)

C



D

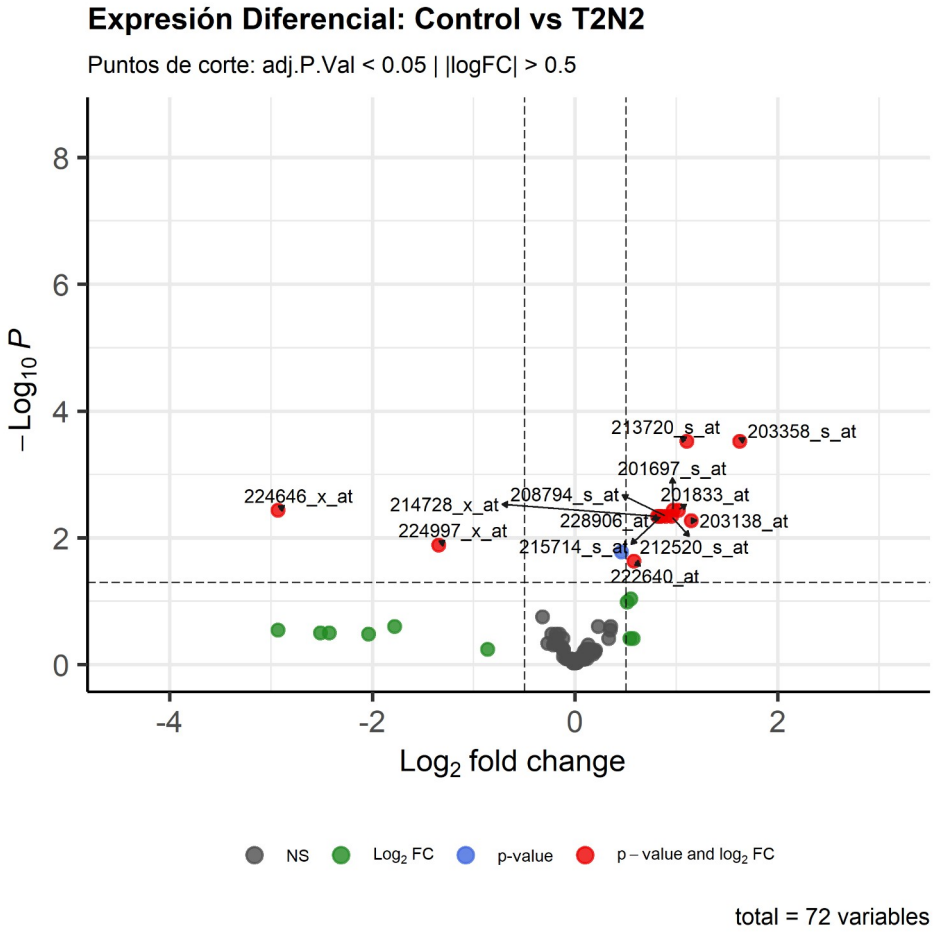
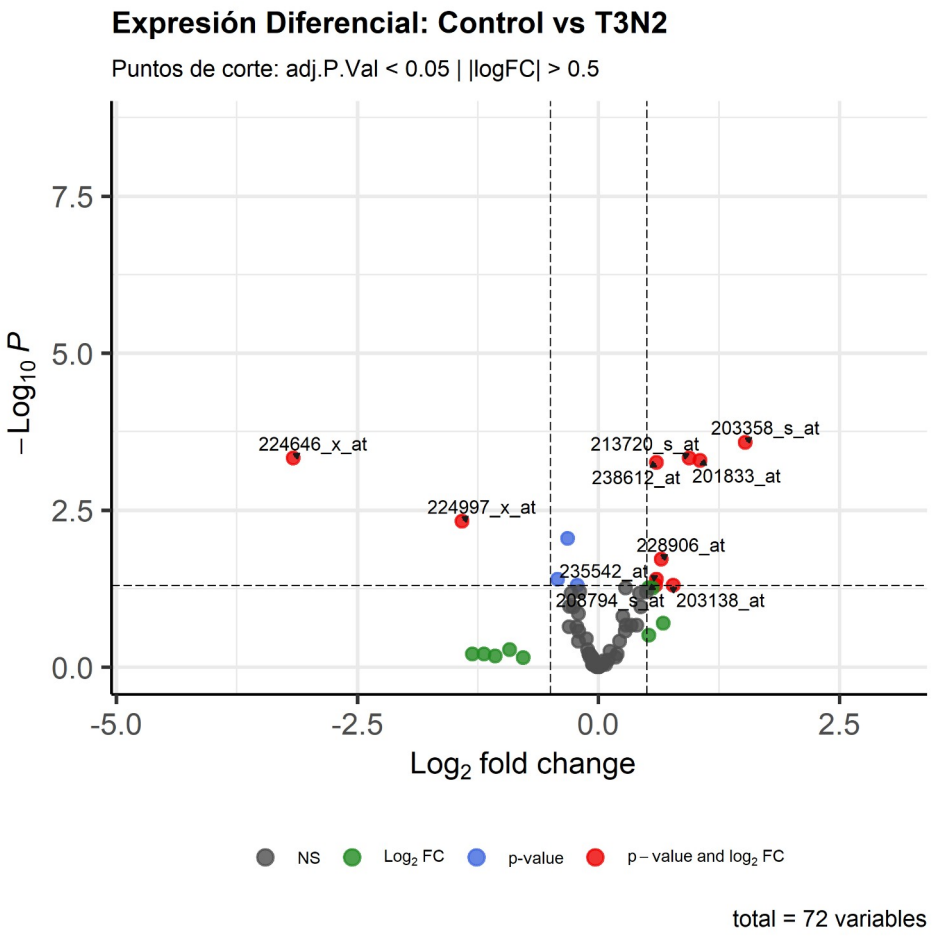


Figure 1 (continued)

E



Volcano plots illustrate the differential expression profiles of core human epigenetic modifiers across consecutive clinical stages compared to healthy controls: **(A)** Control vs. T1N0, **(B)** Control vs. T1N1, **(C)** Control vs. T2N1, **(D)** Control vs. T2N2, and **(E)** Control vs. T3N2. The statistical thresholds for significance are set at an adjusted P-value (adj.P.Val) < 0.05 (horizontal dashed line) and an absolute log2 fold-change (|logFC|) > 0.5 (vertical dashed lines).

Dots are color-coded based on their statistical and biological stringency: grey dots represent non-significant genes (NS); green dots denote genes meeting only the |logFC| threshold; blue dots indicate genes meeting only the P-value criteria; and red dots highlight highly significant core regulators that strictly fulfill both statistical thresholds (adj.P.Val < 0.05 and |logFC| > 0.5).

Key prominent loci are explicitly labeled with their corresponding Affymetrix probe IDs, including the early up-regulation of *EZH2* (probe 203358_s_at) starting at T1N1, the subsequent mobilization of *DNMT1* (201697_s_at) and *SMARCA4* (213720_s_at) at the T2N1 transition, and the synchronized hyperactivation of *HDAC2* (201833_at) operating alongside a profound, multi-stage suppression of the imprinted lncRNA *H19* (224646_x_at) in advanced regional metastatic stages (T2N2 and T3N2). Total variables analyzed per panel = 72.